JOURNAL OF
Materials
CHEMISTRY

Hybrid open frameworks (MIL-*n*). Part 6† Hydrothermal synthesis and X-ray powder *ab initio* structure determination of MIL-11, a series of lanthanide organodiphosphonates with three-dimensional networks, $Ln^{III}H[O_3P(CH_2)_nPO_3]$ ($n=1$–3)

F. Serpaggi and G. Férey*

Institut Lavoisier, UMR CNRS 173, Université de Versailles Saint-Quentin-en-Yvelines, 45, avenue des Etats-Unis, 78035 Versailles Cedex, France. E-mail: ferey@chimie.uvsq.fr

Received 9th April 1998, Accepted 17th September 1998

A series of lanthanide and yttrium propylenediphosphonates has been prepared hydrothermally (210 °C, 4 days) by action of propylenediphosphonic acid on the metal chlorides. The crystal structure of the gadolinium compound $Gd^{III}H[O_3P(CH_2)_3PO_3]$ has been determined *ab initio* from X-ray powder diffraction data and refined by the Rietveld method. The compound crystallizes in the monoclinic space group $C2/m$ (no. 12) with $a=8.2141(3)$ Å, $b=18.9644(8)$ Å, $c=5.2622(2)$ Å, $\beta=111.999(2)^\circ$ and $Z=4$. The final agreement factors are $R_p=0.113$, $R_{wp}=0.142$, Bragg $R=0.050$, $R_F=0.034$ and $\chi^2=1.91$. In the three-dimensional structure, the gadolinium atoms are eight-coordinated. The framework consists of inorganic Gd–P–O sheets joined by organic groups with an interlayer spacing of 9.58 Å. The entire series of the lanthanide elements and yttrium give isotypic structures. Attempts with ethylenediphosphonic acid and gadolinium led to the analogous compound $Gd^{III}H[O_3P(CH_2)_2PO_3]$ which crystallizes in the monoclinic space group $P2_1/c$ (no. 14) with cell parameters $a=5.2918(9)$, $b=15.975(3)$, $c=8.338(1)$ Å, $\beta=111.491(6)^\circ$, $Z=4$ (final agreement factors $R_p=0.078$, $R_{wp}=0.105$, Bragg $R=0.034$, $R_F=0.026$ and $\chi^2=1.50$), and with an interlamellar distance of $d=7.99$ Å. Moreover, the action of methylenediphosphonic acid on La, Ce, Pr and Nd chloride led to a similar structure with a shorter interlamellar distance, $d=7.03$ Å for $Pr^{III}H[O_3P(CH_2)PO_3]$ (space group $C2/m$, with $a=8.3271(4)$, $b=14.0645(7)$, $c=5.3489(3)$ Å, $\beta=111.433(2)^\circ$, $Z=4$, and final agreement factors $R_p=0.092$, $R_{wp}=0.121$, Bragg $R=0.059$, $R_F=0.035$ and $\chi^2=1.98$).

Introduction

The discovery and the structural determination of the ULM-*n* ($n\leqslant 19$) series of oxyfluorinated microporous gallium phosphates by our group six years ago led us to propose a hypothesis for the mechanism of their formation[1] from solution during their templated synthesis. The hypothesis claimed that the oligomers depicted in the solid also exist in the solution and that the charge density of the protonated amine is the driving force of the synthesis, as described in the paper concerning MIL-8 in this issue. (Part 4 in this series.)

We evidenced for the first time some hitherto unknown magnetic microporous iron and vanadium phosphates,[2] in which the total substitution of Ga by Fe or V induces new structural types. Supplementary work is currently in progress in this field with the use of other 3d transition metals. The extension of this idea to microporous rare earth phosphates unfortunately failed owing to the strong affinity of phosphate and fluoride anions towards lanthanide elements which, whatever the chemical conditions, leads to the formation of monazite type phosphates $LnPO_4$ and fluorides LnF_3.

In order to obtain microporous lanthanide compounds, it was then necessary to change our strategy and substitute phosphate anions by other chelating agents which prevent the formation of dense, insoluble inorganic species. This is the case of phosphonates: since the pioneering works of Alberti, Dines and Clearfield, it is well known that these species react with inorganic compounds.[3] Most of the papers concern non-functionalized monophosphonates with the aim of synthesizing layered compounds,[4] but several attempts with diphosphonates led to three-dimensional compounds.[5] We used this idea and we report here the hydrothermal preparation and *ab initio* structural determination of lanthanide and yttrium propylene-, ethylene- and methylene-diphosphonates, which all present a pillared layered structure.

Experimental

Reagents

$LnCl_3\cdot xH_2O$ ($x=6$ or 7) (Aldrich 99.9%), propylenediphosphonic acid (Alfa), ethylene- and methylene-diphosphonic acids (Aldrich) were used, as received, with no further purification.

Preparation of lanthanide and yttrium diphosphonates

The starting mixture, of molar ratio 1 $LnCl_3\cdot xH_2O$: 1 $H_2O_3P(CH_2)_nPO_3H_2$ ($n=1$–3) : 100 H_2O, was placed in a Teflon-lined stainless-steel autoclave and heated at 210 °C for 4 days ($pH_i=1$ and $pH_f=1$). Powders of the product compounds were collected by filtration, washed with distilled water and air dried. The propylenediphosphonates of the whole lanthanide series and Y were prepared and X-ray powder patterns indicate these solids are isotypic with the gadolinium compound. Ethylenediphosphonates of La, Ce, Pr, Nd, Eu, Gd and Yb were prepared; X-ray powder patterns indicate one type of material. Green and white powders were obtained for the Pr and Gd methylenediphosphonates, respectively. X-Ray powder patterns indicate two types of solid: one for La, Ce, Pr and Nd, a second for Eu, Gd and Yb.

X-Ray data collection

Owing to the pseudo-lamellar character of the compounds, the powders were first milled using a McCrone Micronising Mill in order to reduce the size of the particles and to prevent preferred orientation. Step-scanned X-ray powder data for the sample (side-loaded into a flat Mc-Murdie type aluminium

---

†Part 5: preceding paper.

sample holder) were collected on the finely ground sample by means of a Siemens-D5000 computer-automated diffractometer (Cu-Kα, 40 kV, 30 mA). Data were collected between 5 and 60° in 2θ with a step size of 0.02° and a count time of 18 s step^{-1}. The powder patterns were indexed using DICVOL91[6] on the basis of the first 20 observed lines.

For the gadolinium propylenediphosphonate, the best solution which indexed all the lines (figure of merit FOM = 30) indicated a monoclinic unit cell with parameters $a = 8.21(1)$ Å, $b = 18.96(1)$ Å, $c = 5.26(1)$ Å and $\beta = 112.0(1)°$. The systematic absences (hkl: $h+k = 2n$) were consistent with the space group $C2/m$ (no. 12).

For the gadolinium ethylenediphosphonate, the best solution (FOM = 15) led to unit-cell parameters similar to those for the propylenediphosphonate, with reversed a and c parameters and a shorter b parameter: $a = 5.30(1)$ Å, $b = 16.01(1)$ Å, $c = 8.34(1)$ Å, $\beta = 111.6(1)°$. The systematic absences ($h0l$: $l = 2n$; $0k0$: $k = 2n$) were consistent with the space group $P2_1/c$ (no. 14).

For the praseodymium methylenediphosphonate, the best solution (FOM = 30) corresponded to a similar unit-cell with shorter b parameter: $a = 8.33(1)$ Å, $b = 14.06(1)$ Å, $c = 5.35(1)$ Å, $\beta = 111.4(1)°$ (space group $C2/m$). For the gadolinium methylenediphosphonate, the best solution (FOM = 37) indicated cell parameters: $a = 15.75(1)$ Å, $b = 6.61(1)$ Å, $c = 7.03(1)$ Å, $\beta = 121.3(1)°$.

Structure solution and refinement of GdH[$O_3P(CH_2)_3PO_3$]

For better precision concerning the positions and the intensities of the peaks, new data were collected between 7 and 60° and between 60.02 and 100° in 2θ with a step size of 0.02° and a count time of 26 and 52 s step^{-1}, respectively. Initially, the individual reflection intensities were extracted from the powder pattern using the PROFILE program in the DIFFRACT$^{\text{plus}}$ package.[7] Then, background, profile and unit cell parameters were refined using the Rietveld method in the FULLPROF program package.[8] Gadolinium was first located using the direct methods option of the SHELXS program.[9] Phosphorus, oxygen and carbon atoms were then revealed by using FULLPROF and SHELXL together. The structure was refined without any constraints and with an overall isotropic temperature factor. A correction was made for preferred orientation using the usual Rietveld function, with a diffraction vector along the b^*-axis. A final Rietveld refinement plot is given in Fig. 1.

The structure for each lanthanide propylenediphosphonate was refined by FULLPROF with X-ray data collected between 5 and 60° in 2θ (step size = 0.02°, count time = 18 s step^{-1}). After initial refinement of background, profile and cell parameters, the structures were refined with the original coordinates found for GdH[$O_3P(CH_2)_3PO_3$].

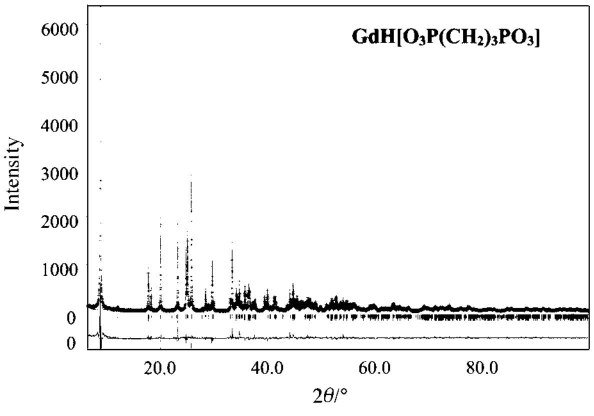

Fig. 1 Observed (+) and calculated (——) profiles for the Rietveld refinement of gadolinium propylenediphosphonate.

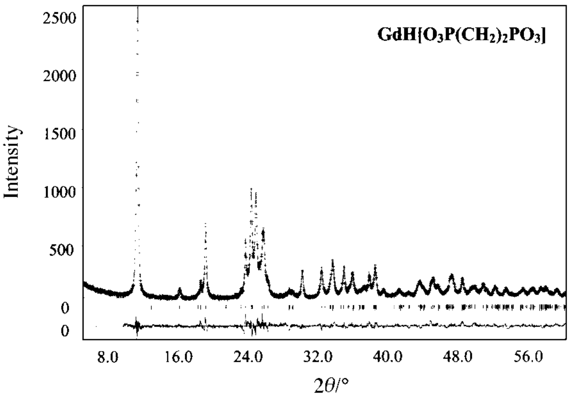

Fig. 2 Observed (+) and calculated (——) profiles for the Rietveld refinement of gadolinium ethylenediphosphonate.

Structure solution and refinement of GdH[$O_3P(CH_2)_2PO_3$]

The procedure is strictly similar to that used for the *ab initio* structure determination of GdH[$O_3P(CH_2)_3PO_3$]. A final Rietveld refinement plot is given in Fig. 2.

Structure solution and refinement of PrH[$O_3P(CH_2)PO_3$]

Considering the similarity of the unit cell to that of GdH[$O_3P(CH_2)_3PO_3$], the structure was readily solved using FULLPROF with X-ray data collected between 7 and 60° and between 60.02 and 100° in 2θ with a step size of 0.02° and a count time of 26 and 52 s step^{-1}, respectively. Background, profile and cell parameters were first refined. The structure was then refined with the positional parameters of GdH[$O_3P(CH_2)_3PO_3$] (except one C atom). A final Rietveld refinement plot is given in Fig. 3.

Full crystallographic details, excluding structure factors, have been deposited at the Cambridge Crystallographic Data Centre (CCDC). See Information for Authors, *J. Mater. Chem.*, 1998, Issue 1. Any request to the CCDC for this material should quote the full literature citation and the reference number 1145/122.

Results

TG analysis under O_2 (heating rate = 5 °C min^{-1}) was carried out for all products. The TG curves indicate the compounds are anhydrous and begin to decompose at 200 °C with a single weight loss. Nevertheless, thermodiffractometry (in air, heating rate + 5 °C min^{-1}) showed that the structure of the compounds is conserved until *ca.* 400 °C. For GdH[$O_3P(CH_2)_3PO_3$], the

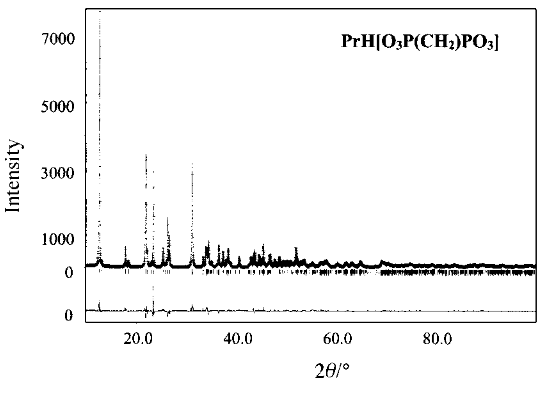

Fig. 3 Observed (+) and calculated (——) profiles for the Rietveld refinement of praseodymium methylenediphosphonate.

Table 1 Crystallographic data for $GdH[O_3P(CH_2)_3PO_3]$, $GdH[O_3P(CH_2)_2PO_3]$ and $PrH[O_3P(CH_2)PO_3]$

	$GdH[O_3P(CH_2)_3PO_3]$	$GdH[O_3P(CH_2)_2PO_3]$	$PrH[O_3P(CH_2)PO_3]$
Formula weight	358.28	344.26	313.89
Crystal system	Monoclinic	Monoclinic	Monoclinic
Space group	$C2/m$ (no. 12)	$P2_1/c$ (no. 14)	$C2/m$ (no. 12)
a/Å	8.2141(3)	5.2918(9)	8.3271(4)
b/Å	18.9644(8)	15.975(3)	14.0645(7)
c/Å	5.2622(2)	8.338(1)	5.3489(3)
β/degrees	111.999(2)	111.491(6)	111.433(2)
V/Å^3	760.04(1)	655.91(1)	583.12(1)
Z	4	4	4
D_c/g cm^{-3}	3.13	3.49	3.57
λ(CuKα_1, Kα_2)/Å	1.5406, 1.5444	1.5406, 1.5444	1.5406, 1.5444
T/°C	20(1)	20(1)	20(1)
No. of reflections	822	379	635
No. of fitted parameters	38	51	35
R_p[a]	0.113	0.078	0.092
R_{wp}[a]	0.142	0.105	0.121
Bragg R[a]	0.050	0.034	0.059
R_F[a]	0.034	0.026	0.035
χ^2[a]	1.91	1.50	1.98

[a] See ref. 8 for definitions.

weight loss is 6.0%. According to X-ray data, the residue (900 °C) is well crystallized monazite type $GdPO_4$, which requires a weight loss of 29.6%. The difference between the observed and calculated weight losses is due to (i) a heavy carbon deposit on the residue and (ii) a too low temperature to allow the volatilization of P_2O_5 and the conversion to $GdPO_4$, as already noted by Clearfield and coworkers for $LaH[O_3PC_6H_5]_2$.[10]

Structure of $GdH[O_3P(CH_2)_3PO_3]$

Crystallographic data are given in Table 1, final positional parameters in Table 2, and bond lengths and angles in Table 3. The structure is a pillared layered one, as seen in Fig. 4(a) and (b). The gadolinium atoms are dodecahedrally coordinated by eight oxygens of the phosphonate groups, as seen in Fig. 5(a) and (b). Each phosphonate group chelates one gadolinium atom and half the chelating oxygen atoms (O1) then bridge to another adjacent gadolinium atom in order to create chains of gadolinium polyhedra along the [100] direction. The third oxygen (O3) bonds to a unique gadolinium atom of an adjacent row and ensures the connection of the chains in order to form inorganic Gd–P–O layers in the (010) plane. The angles formed at the gadolinium atoms by the chelate rings are quite small [O1–Gd–O2, 57.3(7)°] leading to a highly distorted dodecahedron around the gadolinium atom. The P–C bonds point out of the sheets and allow the cross-linking of the inorganic sheets into a three-dimensional structure *via* the organic groups. The unit-cell parameters and volume for each lanthanide (and yttrium) propylenediphosphonate are reported in Table 4. When compared to the lanthanum compound unit cell parameters and volume, the normalized unit-cell parameters and volumes, a/a_{La}, b/b_{La}, c/c_{La} and V/V_{La}, are found to increase with the ionic radii[11] of the lanthanide cation, as shown in Fig. 6. The slight decrease of β with the cation may occur because of slight distortions of the polyhedra *vs.* the lanthanide atom. Finally, owing to the similarity of their ionic radii, yttrium leads to a structure with cell parameters very close to those for $HoH[O_3P(CH_2)_3PO_3]$.

Table 2 Positional parameters for $GdH[O_3P(CH_2)_3PO_3]$

Atom	x	y	z	Site occupation factor
Gd	0	0.2677(1)	0	0.5
P	0.246(1)	0.1506(4)	0.370(2)	
O1	0.299(2)	0.2100(7)	0.222(3)	
O2	0.052(2)	0.1641(6)	0.314(3)	
O3	0.352(2)	0.1526(7)	0.666(3)	
C1	0.220(4)	0	0.359(6)	0.5
C2	0.253(3)	0.064(1)	0.220(5)	

Table 3 Intramolecular distances (Å) and angles (degrees) involving the non-hydrogen atoms of $GdH[O_3P(CH_2)_3PO_3]$[a]

Gd–O1	2.54(1)	Gd–O3^e	2.29(1)
Gd–O1^a	2.54(1)	P–O1	1.52(2)
Gd–O1^b	2.39(2)	P–O2	1.53(2)
Gd–O1^c	2.39(2)	P–O3	1.47(2)
Gd–O2	2.50(1)	P–C2	1.83(2)
Gd–O2^a	2.50(1)	C1–C2	1.49(3)
Gd–O3^d	2.29(1)		
O1–Gd–O1^a	128(1)	O1^c–Gd–O2	118.9(9)
O1–Gd–O1^b	125(1)	O1^c–Gd–O2^a	78.1(7)
O1–Gd–O1^c	64.9(7)	O1^c–Gd–O3^d	76.8(9)
O1–Gd–O2	57.3(7)	O1^c–Gd–O3^e	89.7(9)
O1–Gd–O2^a	82.1(7)	O2–Gd–O2^a	76.3(7)
O1–Gd–O3^d	141(1)	O2–Gd–O3^d	159(1)
O1–Gd–O3^e	77.8(8)	O2–Gd–O3^e	95.8(8)
O1^a–Gd–O1^b	64.9(7)	O2^a–Gd–O3^d	95.8(8)
O1^a–Gd–O1^c	125(1)	O2^a–Gd–O3^e	159(1)
O1^a–Gd–O2	82.1(7)	O3^d–Gd–O3^e	97(1)
O1^a–Gd–O2^a	57.3(7)	O1–P–O2	105(2)
O1^a–Gd–O3^d	77.8(8)	O1–P–O3	111(2)
O1^a–Gd–O3^e	141(1)	O1–P–C2	112(2)
O1^b–Gd–O1^c	160(1)	O2–P–O3	111(2)
O1^b–Gd–O2	78.1(8)	O2–P–C2	105(2)
O1^b–Gd–O2^a	118.9(9)	O3–P–C2	112(2)
O1^b–Gd–O3^d	89.7(9)	P–C2–C1	118(1)
O1^b–Gd–O3^e	76.8(9)	C2–C1–C2^f	109(2)

[a] Symmetry transformations used to generate equivalent atoms: $^a -x, y, -z$; $^b x-1.2, -y+1/2, z$; $^c -x+1/2, -y+1/2, -z$; $^d x-1/2, -y+1/2, z-1$; $^e -x+1/2, -y+1/2, -z+1$; $^f x, -y, z$.

Structure of $GdH[O_3P(CH_2)_2PO_3]$

Crystallographic data are given in Table 1. Final positional parameters and bond lengths and angles are given in Tables 5 and 6, respectively. Symmetry and unit-cell parameters are closely related to those for $GdH[O_3P(CH_2)_3PO_3]$. The structure can be simply deduced from that of $GdH[O_3P(CH_2)_3PO_3]$ by replacing the C_3 chain by the C_2 chain, as shown in Fig. 7(a) and (b). Except for a slight distortion, the inorganic layers remain unchanged [Fig. 8(a) and (b)]. Thus, the main differences between the two structures are (i) that the interlamellar space (along the b axis) is shortened to 7.99 Å, *cf.* 9.56 Å and (ii) that the evenness of the number of carbons in

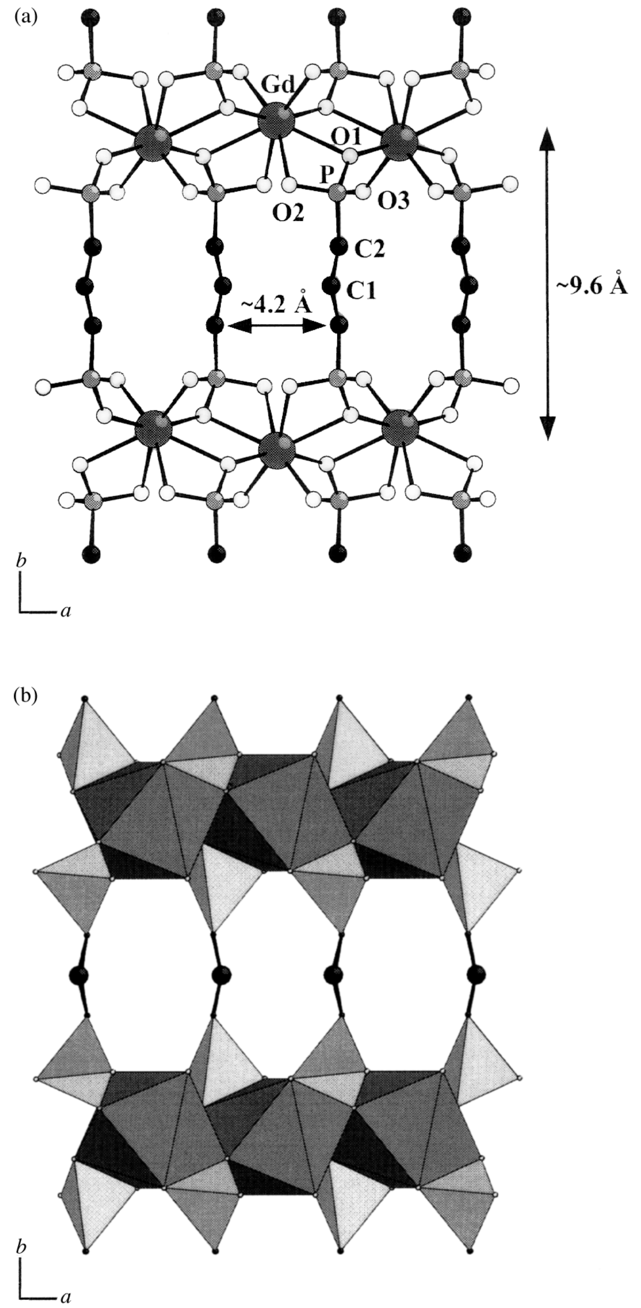

Fig. 4 (a) Projection of the structure of gadolinium propylenediphosphonate down the *c* axis showing a pillared layered structure. (b) Polyhedral drawing of the projected structure of gadolinium propylenediphosphonate down the *c* axis as in (a).

the chain is responsible for a symmetry change ($P2_1/c$ instead of $C2/m$) and a shift of the layers as shown in Fig. 9.

Structure of $PrH[O_3P(CH_2)PO_3]$

Crystallographic data are given in Table 1. Final positional parameters and bond lengths and angles are given in Tables 7 and 8, respectively. The symmetry and unit-cell parameters are closely related to those for $PrH[O_3P(CH_2)_3PO_3]$. The structure can be simply deduced from that of $PrH[O_3P(CH_2)_3PO_3]$ by replacing the C_3 chain by C_1, as shown in Fig. 10(a) and (b). Thus, the main difference between the two structures is that the interlamellar space (along the *b* axis) is shortened to 7.03 Å, *cf.* of 9.56 Å. Because of their poor crystallinity, the structures of the heavier lanthanide compounds still remain unsolved.

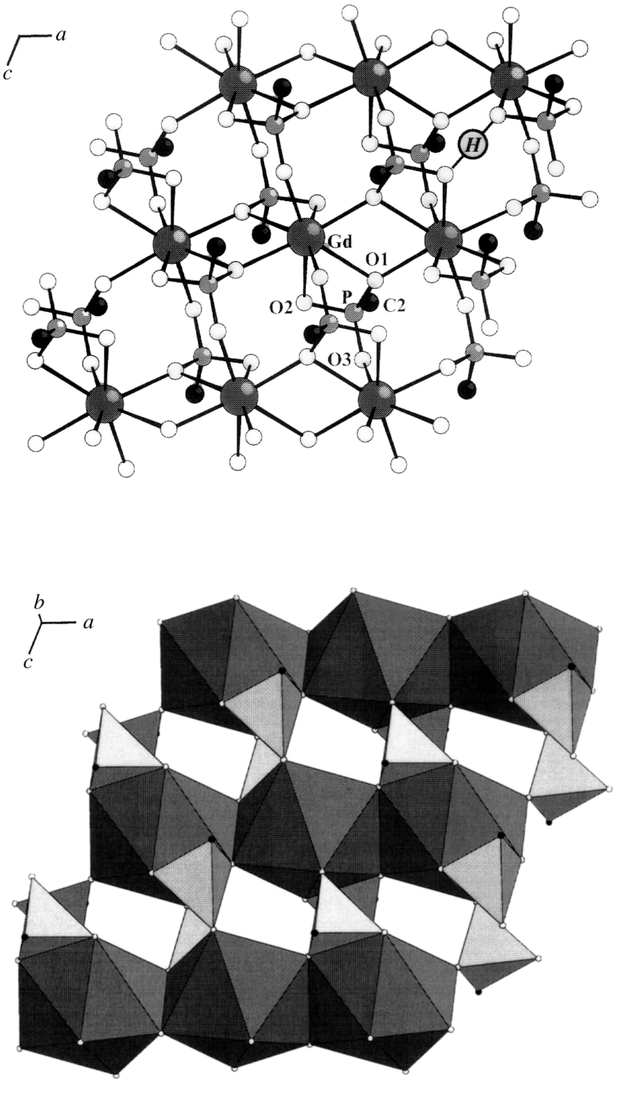

Fig. 5 (a) Layer arrangement in the structure of gadolinium propylenediphosphonate showing the eight-coordinated gadolinium atoms; the acid proton is evidenced within the circle. (b) Polyhedral representation of the inorganic layer in propylenediphosphonate showing the arrangement of Gd and P atoms polyhedra.

Table 4 Evolution of the cell parameters and volume of $LnH[O_3P(CH_2)_3PO_3]$ *vs.* the lanthanide element, and cell parameters and volume for $YH[O_3P(CH_2)_3PO_3]$

Element	*a*/Å	*b*/Å	*c*/Å	*β*/degrees	*V*/Å^3
La	8.435(1)	19.216(2)	5.358(1)	111.53(1)	807.9(1)
Ce	8.389(1)	19.153(2)	5.334(1)	111.63(1)	796.6(1)
Pr	8.348(1)	19.112(2)	5.321(1)	111.72(1)	788.7(1)
Nd	8.312(1)	19.075(1)	5.308(1)	111.80(1)	781.3(1)
Sm	8.258(1)	19.014(1)	5.284(1)	111.91(1)	769.7(1)
Eu	8.232(1)	18.982(1)	5.270(1)	111.95(1)	763.9(1)
Gd	8.214(1)	18.964(1)	5.262(1)	112.00(1)	754.6(1)
Tb	8.190(1)	18.928(1)	5.244(1)	112.03(1)	753.7(1)
Dy	8.171(1)	18.899(1)	5.231(1)	112.03(1)	748.7(1)
Ho	8.153(1)	18.873(1)	5.221(1)	112.09(1)	744.4(1)
Er	8.138(1)	18.848(2)	5.209(1)	112.10(1)	740.3(1)
Tm	8.120(1)	18.826(1)	5.201(1)	112.10(1)	736.6(1)
Yb	8.102(1)	18.798(1)	5.183(1)	112.11(1)	731.4(1)
Lu	8.095(1)	18.787(2)	5.176(1)	112.17(1)	729.0(1)
Y	8.156(1)	18.867(1)	5.221(1)	112.04(1)	744.8(1)

Discussion

Prior to this study, only two layered lanthanide phosphonates were structurally characterized. Indeed, five years ago, while studying a series of phenyl- and benzyl-phosphonates of the

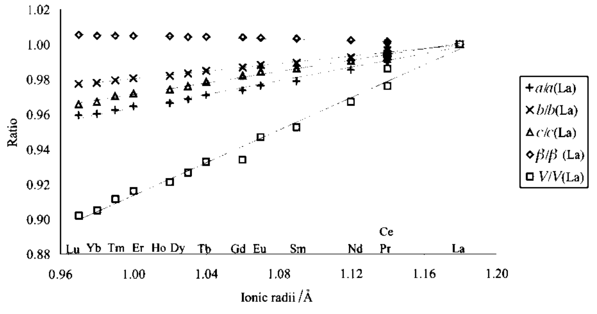

Fig. 6 Curves showing the evolution of the normalized unit-cell parameters and volume of $LnH[O_3P(CH_2)_3PO_3]$ *vs.* the ionic radii of the lanthanide elements Ln (normalized parameter = parameter for Ln/parameter for La).

Table 5 Positional parameters for $GdH[O_3P(CH_2)_2PO_3]$

Atom	*x*	*y*	*z*
Gd	0.7816(9)	0.2255(2)	0.2152(6)
P1	0.415(4)	0.1411(8)	0.477(2)
P2	0.139(3)	0.375(1)	0.455(2)
O1	0.114(6)	0.340(2)	0.279(4)
O2	−0.044(7)	0.315(2)	0.495(4)
O3	0.136(6)	0.128(2)	0.391(4)
O4	0.572(5)	0.212(2)	0.404(2)
O5	0.461(7)	0.348(2)	0.155(4)
O6	0.456(6)	0.377(2)	0.571(4)
C1	0.428(6)	−0.039(1)	0.489(7)
C2	0.06(1)	0.484(2)	0.440(5)

Table 6 Intramolecular distances (Å) and angles (degrees) involving the non-hydrogen atoms of $GdH[O_3P(CH_2)_2PO_3]^a$

Gd–O1^a	2.45(3)	P1–O4	1.64(3)
Gd–O2^a	2.60(3)	P1–O5^d	1.43(3)
Gd–O2^b	2.42(3)	P1–C1^e	1.81(3)
Gd–O3^a	2.46(3)	P2–O1	1.53(4)
Gd–O4	2.25(3)	P2–O2	1.48(4)
Gd–O4^c	2.62(2)	P2–O6	1.60(4)
Gd–O5	2.51(3)	P2–C2	1.79(3)
Gd–O6^c	2.37(3)	C1–C1^e	1.43(3)
P1–O3	1.40(4)	C2–C2^f	1.45(7)
O1^a–Gd–O2^a	54(1)	O3^a–Gd–O6^c	97(2)
O1^a–Gd–O2^b	85(2)	O4–Gd–O4^c	126(1)
O1^a–Gd–O3^a	91(2)	O4–Gd–O5	75(2)
O1^a–Gd–O4	115(2)	O4–Gd–O6^c	80(2)
O1^a–Gd–O4^c	87(2)	O4^c–Gd–O5	60(1)
O1^a–Gd–O5	81(2)	O4^c–Gd–O6^c	78(2)
O1^a–Gd–O6^c	163(2)	O5–Gd–O6^c	97(2)
O2^a–Gd–O2^b	136(2)	O3–P1–O4	12(4)
O2^a–Gd–O3^a	83(2)	O3–P1–O5^d	107(4)
O2^a–Gd–O4	62(1)	O3–P1–C1^e	106(3)
O2^a–Gd–O4^c	124(2)	O4–P1–O5^d	112(3)
O2^a–Gd–O5	75(2)	O4–P1–C1^e	115(2)
O2^a–Gd–O6^c	142(2)	O5^d–P1–C1^e	93(3)
O2^b–Gd–O3^a	82(2)	O1–P2–O2	98(3)
O2^b–Gd–O4	158(2)	O1–P2–O6	107(3)
O2^b–Gd–O4^c	60(1)	O1–P2–C2	111(3)
O2^b–Gd–O5	118(2)	O2–P2–O6	120(4)
O2^b–Gd–O6^c	81(2)	O2–P2–C2	120(3)
O3^a–Gd–O4	89(2)	O6–P2–C2	101(3)
O3^a–Gd–O4^c	142(2)	P1–C1–C1^e	125(2)
O3^a–Gd–O5	157(2)	P2–C2–C2^f	116(4)

^{a}Symmetry transformations used to generate equivalent atoms: $^a x+1, y, z$; $^b x+1, -y+1/2, z-1/2$; $^c x, -y+1/2, z-1/2$; $^d x, -y+1/2, z+1/2$; $^e -x+1, -y, -z+1$; $^f -x, -y+1, -z+1$.

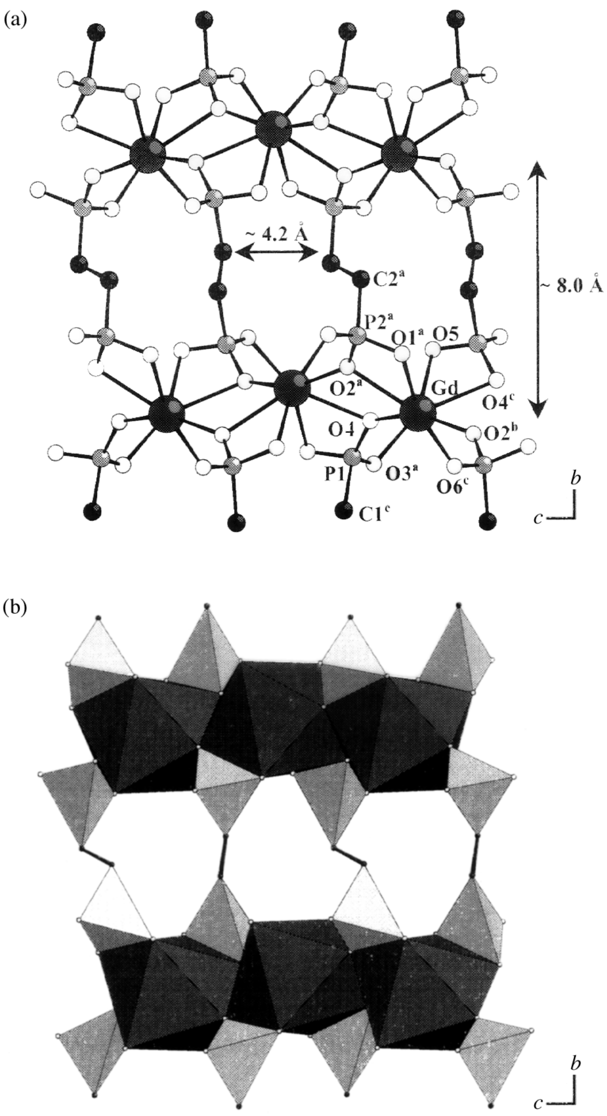

Fig. 7 (a) Projection of the structure of gadolinium ethylenediphosphonate down the *a* axis showing a pillared layered structure closely related to that of gadolinium propylenediphosphonate. (b) Polyhedral drawing of the projected structure of gadolinium ethylenediphosphonate down the *a* axis as in (a).

lanthanide elements, Clearfield and coworkers obtained crystals of the lanthanum compounds, $La[O_3PC_6H_5][HO_3PC_6H_5]$ and $La[O_3PCH_2C_6H_5][HO_3PCH_2C_6H_5]{\cdot}2H_2O$, and solved their crystal structures.[10]

After Clearfield sent us the correct coordinates for $La[O_3PC_6H_5][HO_3PC_6H_5]$, it appeared that the structure of the new pillared layered $LnH[O_3P(CH_2)_nPO_3]$ **1** is closely related to that of the layered $La[O_3PC_6H_5][HO_3PC_6H_5]$ **2**. As shown in Table 9, except for the different *b* parameter and symmetry (due to the different organic groups), the unit-cell parameters are almost the same. Vectors of the unit cell for **2** can be deduced from those for **1** by roughly applying the transformation matrix.

$$\begin{pmatrix} -1 & 0 & -1 \\ 0 & -1 & 0 \\ 0 & 0 & 1 \end{pmatrix}$$

When correctly re-oriented, the structures look the same and in both case the inorganic layers are strictly similar. The whole arrangement of the Ln, P and O atoms within the layer is the same and bond lengths and angles in $LnH[O_3P(CH_2)_3PO_3]$ are consistent with those observed in $La[O_3PC_6H_5][HO_3PC_6H_5]$. Clearfield and coworkers prepared $La[O_3PC_6H_5][HO_3PC_6H_5]$ at low pH (≈2), and thus they obtained an acidic phosphonate ($La[O_3PC_6H_5][HO_3PC_6H_5]$ which can be rewritten $LaH[O_3PC_6H_5]_2$).[10] Nevertheless, they could not locate the proton in the Fourier difference maps. But after

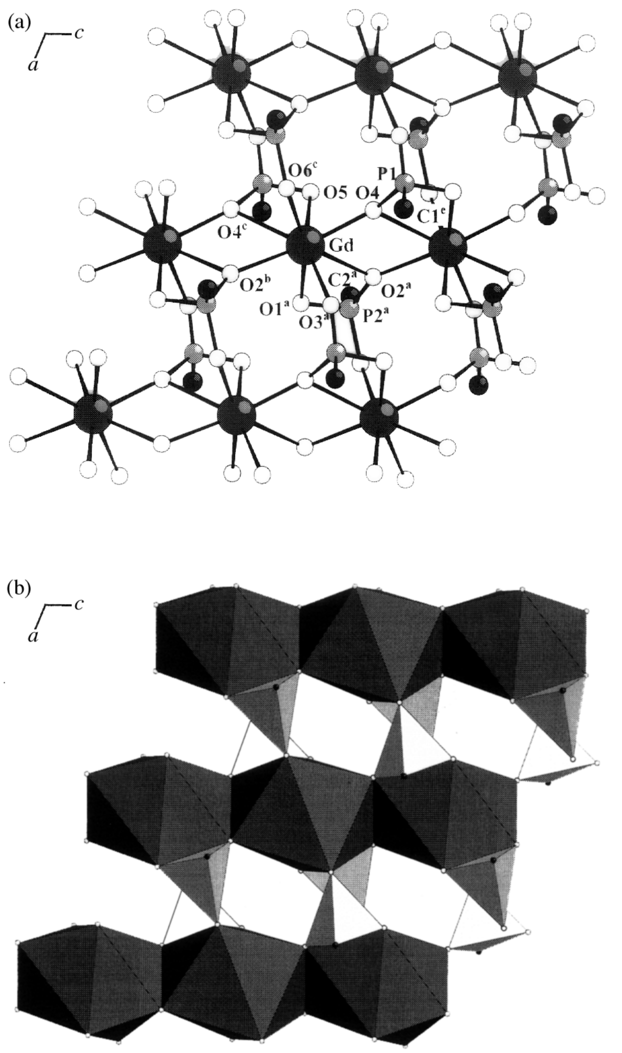

Fig. 8 (a) Layer arrangement in the structure of gadolinium ethylenediphosphonate similar to the arrangement in the gadolinium propylenediphosphonate shown in Fig. 5(a). (b) Polyhedral representation of the inorganic layer in ethylenediphosphonate showing the arrangement of Gd and P atoms polyhedra.

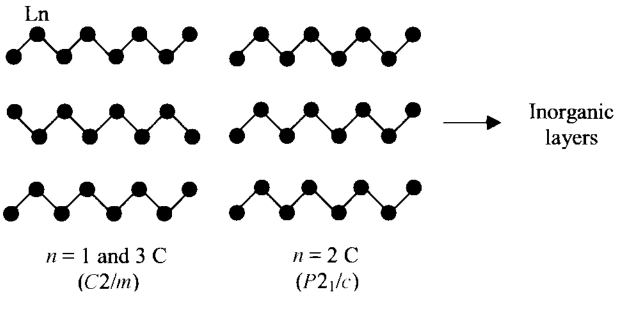

Fig. 9 Effect of the parity of the number of carbon atoms in the chain on the layout of the inorganic sheets.

Table 7 Positional parameters for $PrH[O_3P(CH_2)PO_3]$

Atom	*x*	*y*	*z*	Site occupation factor
Pr	0	0.2739(1)	0	0.5
P	0.241(1)	0.1148(3)	0.356(1)	
O1	0.282(1)	0.2003(7)	0.181(2)	
O2	0.055(1)	0.1294(5)	0.330(2)	
O3	0.355(1)	0.1134(6)	0.657(2)	
C	0.253(3)	0	0.226(4)	0.5

Table 8 Intramolecular distances (Å) and angles (degrees) involving the non-hydrogen atoms of $PrH[O_3P(CH_2)PO_3]^a$

Pr–O1	2.42(1)	Pr–O3^d	2.39(1)
Pr–O1^a	2.42(1)	Pr–O3^e	2.39(1)
Pr–O1^b	2.38(2)	P–O1	1.63(1)
Pr–O1^c	2.38(2)	P–O2	1.52(1)
Pr–O2	2.62(1)	P–O3	1.54(1)
Pr–O2^a	2.62(1)	P–C	1.77(9)
O1–Pr–O1^a	129.4(7)	O1^c–Pr–O2	114.9(6)
O1–Pr–O1^b	132.5(8)	O1^c–Pr–O2^a	79.3(5)
O1–Pr–O1^c	56.9(5)	O1^c–Pr–O3^d	80.5(6)
O1–Pr–O2	59.6(5)	O1^c–Pr–O3^e	87.9(6)
O1–Pr–O2^a	80.9(5)	O2–Pr–O2^a	78.3(4)
O1–Pr–O3^d	137.3(7)	O2–Pr–O3^d	161.0(6)
O1–Pr–O3^e	80.4(5)	O2–Pr–O3^e	94.8(5)
O1^a–Pr–O1^b	56.9(5)	O2^a–Pr–O3^d	94.8(5)
O1^a–Pr–O1^c	132.5(8)	O2^a–Pr–O3^e	161.0(6)
O1^a–Pr–O2	80.9(5)	O3^d–Pr–O3^e	96.9(6)
O1^a–Pr–O2^a	59.6(5)	O1–P–O2	105(1)
O1^a–Pr–O3^d	80.4(5)	O1–P–O3	116(1)
O1^a–Pr–O3^e	137.3(7)	O1–P–C	113.1(7)
O1^b–Pr–O1^c	162.5(8)	O2–P–O3	108(1)
O1^b–Pr–O2	79.3(5)	O2–P–C	107(1)
O1^b–Pr–O2^a	114.9(6)	O3–P–C	107(1)
O1^b–Pr–O3^d	87.9(6)	P–C–P^f	131.0(6)
O1^b–Pr–O3^e	80.5(6)		

[a] Symmetry transformations used to generate equivalent atoms: ^{a} $-x$, y, $-z$; ^{b} $x-1/2$, $-y+1/2$, z; ^{c} $-x+1/2$, $-y+1/2$, $-z$; ^{d} $x-1/2$, $-y+1/2$, $z-1$; ^{e} $-x+1/2$, $-y+1/2$, $-z+1$; ^{f} x, $-y$, z.

examination of the P–O lengths [two two-coordinated oxygen atoms, O*, form slighty longer P–O* bonds and are separated by a distance of 2.41(1) Å] and ^{31}P MAS NMR analysis, they found the proton to be either randomly distributed between the O* oxygen atoms or equidistant between them. As no single crystals of $LnH[O_3P(CH_2)_3PO_3]$ could be obtained, the structure was determined *ab initio* and no hydrogen atom could be located in the Fourier difference maps. However, since the $LnH[O_3P(CH_2)_nPO_3]$ compounds were prepared at low pH (=1) and are analoguous to $LaH[O_3PC_6H_5]_2$, they should also be acidic. In $GdH[O_3P(CH_2)_3PO_3]$, two-coordinated O2 atoms form P–O2 bonds of 1.53(2) Å and are separated by a distance of 2.41(2) Å. Thus, one can easily imagine one acid proton either randomly distributed between the O2 oxygen atoms or equidistant between them [Fig. 5(a)], as in $LaH[O_3PC_6H_5]_2$. Moreover, this added proton satisfies the electroneutrality of the structure.

Conclusion

In order to obtain microporous lanthanide compounds, we investigated the system rare-earth/diphosphonic acid. Until now, the only lanthanide phosphonates to be reported were layered due to the use of a non-functionalized monophosphonic acid as a precursor.[10,12] By using diphosphonic acids, we were able to prepare and characterize pillared layered

Table 9 Comparison between crystallographic data for $La[O_3PC_6H_5][HO_3PC_6H_5]$ and $LaH[O_3P(CH_2)_3PO_3]$

	$La[O_3PC_6H_5][HO_3PC_6H_5]$ (small cell[11])	$LaH[O_3P(CH_2)_3PO_3]$
Formula weight	452.07	339.94
Crystal system	Triclinic	Monoclinic
Space group	$P\bar{1}$ (no. 2)	$C2/m$ (no. 12)
a/Å	8.410(3)	8.4348(7)
b/Å	15.696(7)	19.216(2)
c/Å	5.636(1)	5.3584(5)
α/degrees	90.24(3)	90.0
β/degrees	108.99(1)	111.530(5)
γ/degrees	85.59(4)	90.0
V/Å^3	701.3(4)	807.9(1)

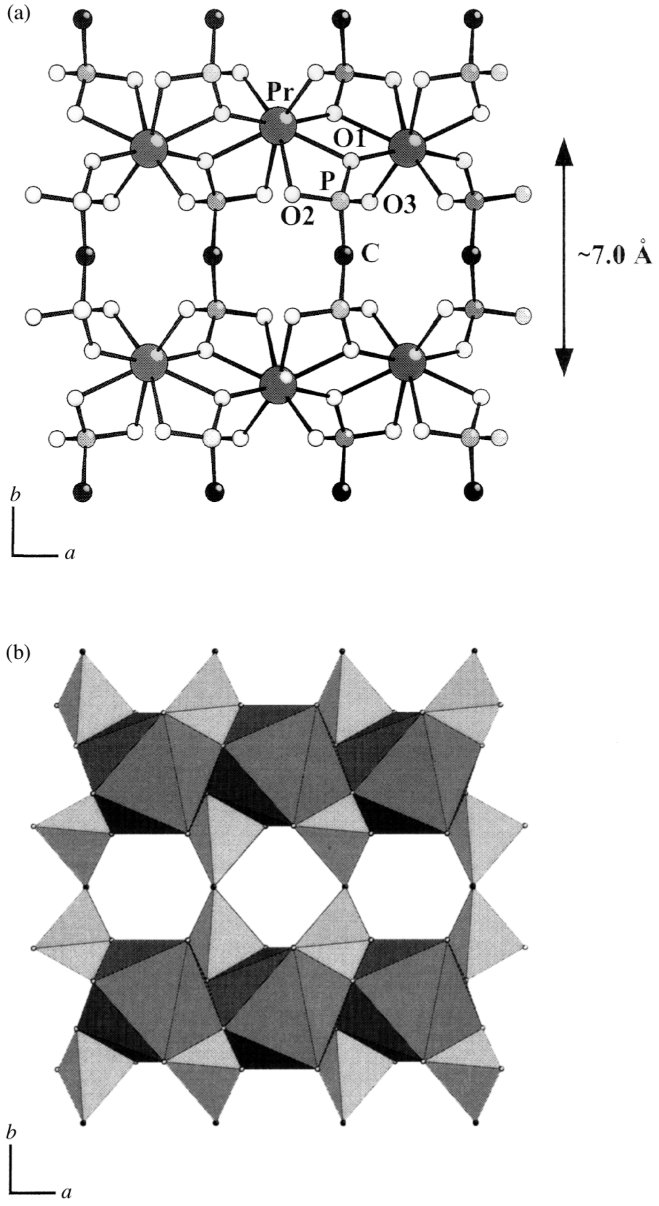

Fig. 10 (a) Projection of the structure of praseodymium methylenediphosphonate down the *c* axis showing a pillared layered structure closely related to that of gadolinium propylenediphosphonate. (b) Polyhedral drawing of the projected structure of praseodymium methylenediphosphonate down the *c* axis as in (a).

lanthanide diphosphonates. The inorganic layers are the same in all the layered compounds, as discussed above, but the diphosphonate replaces the dangling organic groups in order to cross-link the sheets. Unfortunately, in this series, the short distance between adjacent lanthanide atoms in the inorganic layer (*ca.* 4.2 Å), and therefore between the carbon chains, does not give rise to any porosity. In order to generate porosity, attempts are currently in progress using the coprecipitation of phosphate (or phosphite) and phosphonate groups described by Alberti *et al.*[5a,b] In this way, the phosphate groups may act as spacers between the pillared phosphonates and generate the desired porosity.

Acknowledgments

The authors are grateful to Rhône-Poulenc for financial support and to Professor Abraham Clearfield for providing us the correct coordinates of the structure of La[$O_3PC_6H_5$][$HO_3PC_6H_5$].

References

1 G. Férey, *J. Fluorine Chem.*, 1995, **72**, 187; *C. R. Acad. Sci. Sér. C*, 1998, **2**, and references therein.
2 D. Riou and G. Férey, *J. Solid State Chem.*, 1994, **111**, 422; D. Riou, F. Taulelle, and G. Férey, *Inorg. Chem.*, 1996, **35**, 6392; M. Cavellec, D. Riou, C. Ninclaus, J.-M. Grenèche and G. Férey, *Zeolites*, 1996, **17**, 250; M. Cavellec, D. Riou, J.-M. Grenèche and G. Férey, *J. Magn. Magn. Mater.*, 1996, **163**, 173; M. Cavellec, J.-M. Grenèche, D. Riou and G. Férey, *Microporous Mater.*, 1997, **8**, 103; M. Cavellec, J.-M. Grenèche and G. Férey, *Microporous Mater.*, 1998, **20**, 45; M. Cavellec, C. Egger, J. Linares, M. Nogues, F. Varret and G. Férey, *J. Solid State Chem.*, 1997, **134**, 349.
3 A. Clearfield, *Curr. Opin. Solid State Mater. Sci.*, 1996, **1**, 268 and references therein.
4 M. E. Thompson, *Chem. Mater.*, 1994, **6**, 1168 and references therein.
5 (*a*) G. Alberti, U. Costantino, F. Marmottini, R. Vivani and P. Zappelli, *Angew. Chem., Int. Ed. Engl.*, 1993, **32**, 1357; (*b*) G. Alberti, F. Marmottini, S. Murcia-Mascarós and R. Vivani, *Angew. Chem., Int. Ed. Engl.*, 1994, **33**, 1594; (*c*) L. A. Vermeulen and M. E. Thompson, *Chem. Mater.*, 1994, **6**, 77; (*d*) V. Soghomonian, Q. Chen, R. C. Haushalter and J. Zubieta, *Angew. Chem., Int. Ed. Engl.*, 1995, **34**, 223; (*e*) V. Soghomonian, R. Diaz, R. C. Haushalter, C. J. O'Connor and J. Zubieta, *Inorg. Chem.*, 1995, **34**, 4460; (*f*) H. Byrd, A. Clearfield, D. Poojary, K. P. Reis and M. E. Thompson, *Chem. Mater.*, 1996, **8**, 2239; (*g*) D. M. Poojary, B. Zhang, P. Bellinghausen and A. Clearfield, *Inorg. Chem.*, 1996, **35**, 4942; (*h*) D. M. Poojary, B. Zhang, P. Bellinghausen and A. Clearfield, *Inorg. Chem.*, 1996, **35**, 5254; (*i*) G. Bonavia, R. C. Haushalter, C. J. O'Connor and J. Zubieta, *Inorg. Chem.*, 1996, **35**, 5603; (*j*) P. J. Zapf, D. J. Rose, R. C. Haushalter and J. Zubieta, *J. Solid State Chem.*, 1996, **125**, 182; (*k*) D. L. Lohse and S. C. Sevov, *Angew. Chem., Int. Ed. Engl.*, 1997, **36**, 1619.
6 A. Boultif and D. Loüer, *J. Appl. Crystallogr.*, 1991, **24**, 987.
7 Siemens AG, DIFFRACT^{plus}, Karlsruhe, Germany, 1996.
8 J. Rodriguez-Carjaval, in *Collected Abstracts of Powder Diffraction Meeting, Toulouse, France*, 1990, p. 127.
9 G. M. Sheldrick, *Siemens Analytical X-ray Instruments*, 1994.
10 R.-C. Wang, Y. Zhang, H. Hu, R. R. Frausto and A. Clearfield, *Chem. Mater.*, 1992, **4**, 864.
11 R. D. Shannon, *Acta Crystallogr., Sect. A*, 1974, **32**, 751.
12 G. Cao, V. M. Lynch, J. S. Swinnea and T. E. Mallouk, *Inorg. Chem.*, 1990, **29**, 2112.

Paper 8/02715C